4f and 6f processes at e^+e^- colliders.

E. Migliore[a]

[a]Dipartimento di Fisica Sperimentale dell'Università di Torino and INFN Sezione di Torino, via P. Giuria 1, 10125 Turin, Italy

The running of LEP at centre-of-mass energy $\sqrt{s} \approx 200$ GeV offered the first opportunity to study 4f processes in e^+e^- collisions. The experimental results and the theoretical achievements in the field are reviewed together with their relevance for the future Linear Collider.

1. 4f physics

4f physics is the measurement of the cross-section for the reaction $e^+e^- \to 4f$. As such it covers a broad set of processes at LEP, essentially every final state which is not a two-fermion ($e^+e^- \to f\bar{f}(\gamma)$) or a multi-photon ($e^+e^- \to \gamma\gamma(\gamma)$) final state. According to Quantum Field Theory (QFT) the complete set of Feynman diagrams is required to describe properly the reaction $e^+e^- \to 4f$. On the other hand 4f processes are usually classified on the basis of "quasi on-shell" representation of the process itself, where intermediate states are produced which later decay into that particular final state: $\sigma(e^+e^- \to 4f) = \sigma(e^+e^- \to X) \times BR(X \to 4f)$.
According to this description the following 4f processes can be identify:

- WW production;
- $e^+e^-f\bar{f}$ production via multiperipheral graphs;
- ZZ production;
- Weν production (single-W);
- γ^*/Zee production (single-γ^*/Z).

Among the processes listed above only ZZ, single-W and single-Z production will be discussed in this report. A detailed description of WW production and of multiperipheral processes can be found in refs. [1] and [2].
The cross-section as a function of the centre-of-mass energy $\sqrt{s}$ for the most relevant processes is shown in figure 1 [3].
LEP offered during its running at high energy (LEP2) a unique opportunity to study these processes, as it delivered more that 600 pb^{-1} of integrated luminosity per experiment, reaching $\sqrt{s}$ up to 209 GeV (cf. table 1).

Table 1
The running of LEP at high energy.

$\sqrt{s}$ (GeV)	183	189	192-202	205	>207
$\mathcal{L}_{\text{int}}$ (pb^{-1})	55	170	230	75	130

The relevance of 4f physics is obviously related to the hunting for new physics signals during the LEP2 run. In fact 4f physics deals with final states which allow different interpretations. This is the case in instance of the $e^+e^-b\bar{b}$ final state which at the same time is a golden channel for Higgs boson discovery but it can also originate from a ZZ or Zee process. Furthermore, as the 4f cross-sections are defined with just a subset of the Feynman diagrams, they usually have a larger sensitivity to anomalies in the Standard Model (SM) couplings. However 4f physics at LEP2 is interesting in itself as, for the first time, SM processes that will be those dominant for precision electroweak physics at the future Linear Collider were studied.
A complete review of the experimental results and of the theoretical achievements in 4f physics can

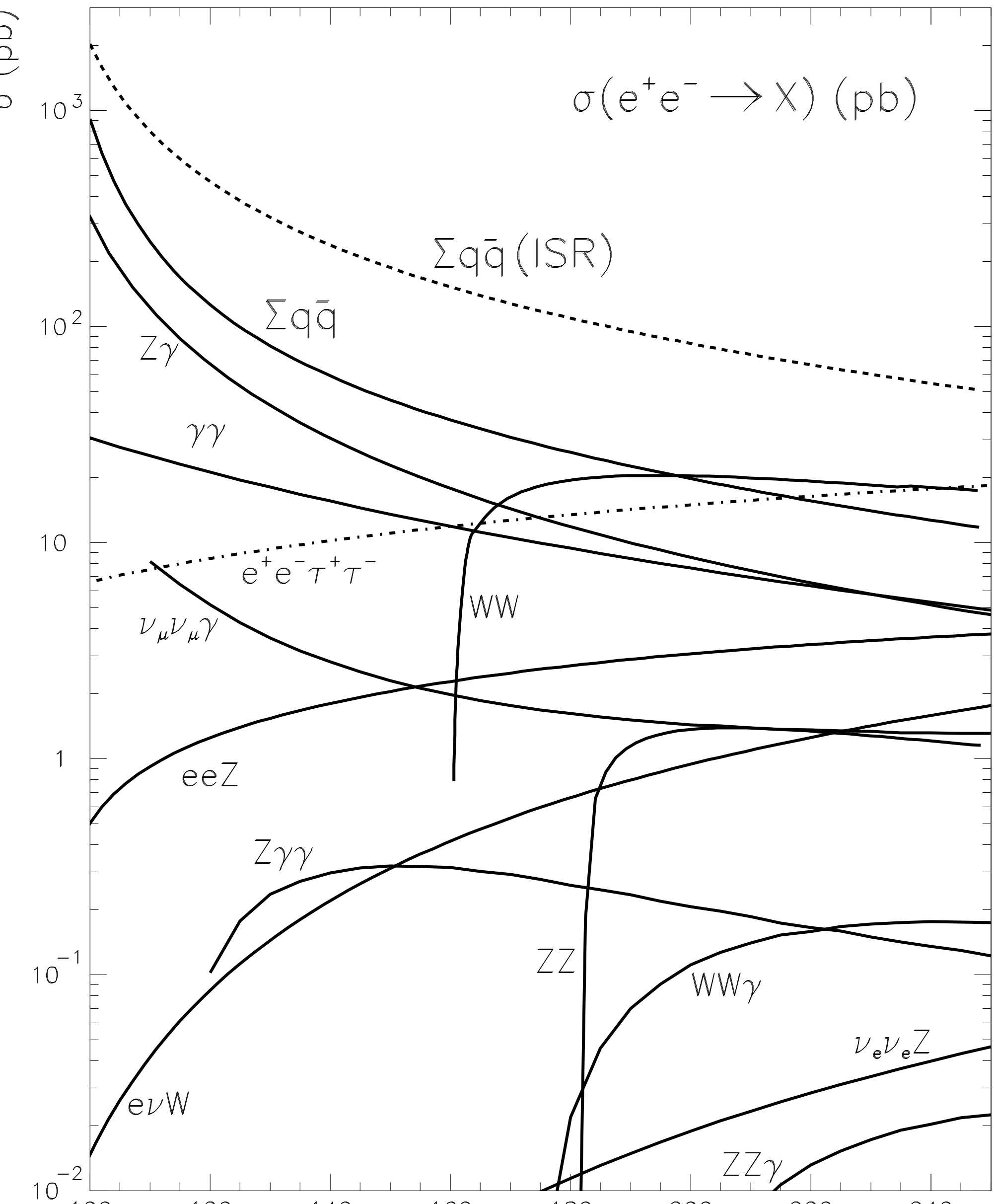

Figure 1. Cross-section for some typical Standard Model processes. For $e^+e^- \rightarrow e^+e^-Z, e^-\bar{\nu}_e W^+ + e^+\nu_e W^-, \nu_e\bar{\nu}_e Z$, only the t-channel contribution is shown (from ref. [3]).

Table 2
Final states experimentally investigated for ZZ.

Final state	Signature	BR	ε (efficiency)	p (purity)	$BR \times \varepsilon \times p$
$q\bar{q}q\bar{q}$ (q$\neq$b)	4 jets	30%	30%	30%	3%
$q\bar{q}b\bar{b}$	4 jets+b-tag	19%	40%	70%	5%
$q\bar{q}\ell^+\ell^-$	2 jets+2 leptons	14%	60%	85%	7%
$q\bar{q}\nu\bar{\nu}$	2 jets+E_{miss}	28%	35%	60%	6%
$\ell^+\ell^-\ell^+\ell^-$	4 leptons	1%	55%	65%	0.3%
$\ell^+\ell^-\nu\bar{\nu}$	2 leptons+E_{miss}	4%	40%	70%	1%

be found in refs. [4] and [5] respectively.

1.1. ZZ production

The ZZ cross-section is defined by the two diagrams shown in figure 2 (NC02) with all the decay modes allowed for both Z bosons. Non-NC02 contributions to the same 4f final state and their interference with NC02 are considered as background. A subtle point in the definition concerns final states with 4 identical fermions, i.e. $Z(\to f_1\bar{f}_1)Z(\to f_2\bar{f}_2)$ with $f_1 = f_2$. In this case crossings of fermions from the two Z's, i.e. $f_1\bar{f}_2$, are neglected as in general non double-resonant.

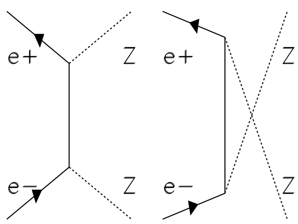

Figure 2. Feynman diagrams for on-shell ZZ production (referred to as NC02 graphs).

Theory. There are no singularities in the calculation of the ZZ cross-section. An $\mathcal{O}(\alpha)$ calculation in the double-pole approximation, as for the CC03 cross-section, is in principle feasible but it has not been done yet as the statistical significance of this measurement is lower than for WW cross-section ($\sigma_{WW}/\sigma_{ZZ} \approx 20$). An overall 2% accuracy in the calculation is estimated, resulting from the change of the renormalization scheme and the implementation of the QED corrections.
Experiment. The final states experimentally investigated are listed in table 2. Considering as a figure of merit the product $BR \times \varepsilon \times p$ one can observe that the combined result actually receives relevant contributions from several final states. Each LEP experiment provides one value of σ_{ZZ} for each energy point. This is extracted from a global likelihood fit of discriminant variables, for channels like $q\bar{q}q\bar{q}$ or $q\bar{q}\nu\bar{\nu}$, and Poissonian probabilities, for channels with events counting like $q\bar{q}\ell^+\ell^-$ or $q\bar{q}\nu\bar{\nu}$. These values are then combined among the four experiments, weighted by the symmetrized expected statistical error. A general good agreement between data and expectations is observed in each channel and for each experiment. At $\sqrt{s} = 189$ GeV, the centre-of-mass energy where the largest luminosity was accumulated ($\approx 150\ \mathrm{pb}^{-1}$ per experiment), the combined result is:

$$\begin{aligned}\sigma_{ZZ} &= 0.90 \pm 0.07(\mathrm{stat}) \pm 0.03(\mathrm{syst}) \\ &\quad \pm 0.02(\mathrm{com\,syst})\,\mathrm{pb}.\end{aligned}$$

The excitation curve for σ_{ZZ} is shown in figure 3. Because of its relevance as a background in the Higgs search, L3 and OPAL measure the b-quark content in ZZ production adding the information of the b-tag variable in the $q\bar{q}\nu\bar{\nu}$ and $q\bar{q}\ell^+\ell^-$ channels. Both the experiments find results in agreement with the SM predictions.
Releasing a constraint on $m_{f\bar{f}}$ DELPHI measures the cross-section for $Z\gamma^*$ production. The channels experimentally investigated are listed in

Table 3
Final states experimentally investigated for $Z\gamma^*$.

Final state	Signature	ε	$\sigma_{Z\gamma^*}$ (pb)
$q\bar{q}\ell^+\ell^-$ ($\ell = \mu, e$)	$Z\gamma^*$ dominating at low $m_{\ell^+\ell^-}$	35%	$0.129 \pm 0.020 \pm 0.008$
$q\bar{q}\nu\bar{\nu}$	monojet topology ($Z \to \nu\bar{\nu}$)	31%	$0.219 \pm 0.035 \pm 0.015$
$q\bar{q}q\bar{q}$	$q\bar{q}\rho(\to \pi^+\pi^-)$	18%	$0.071 \pm 0.042 \pm 0.015$
$\ell^+\ell^-\ell^+\ell^-$	mainly $e^+e^-\mu^+\mu^-$	15%	0.052 ± 0.016

table 3. The expected cross-sections are about 0.1 pb. Good agreement with SM expectations is found for all the channels.

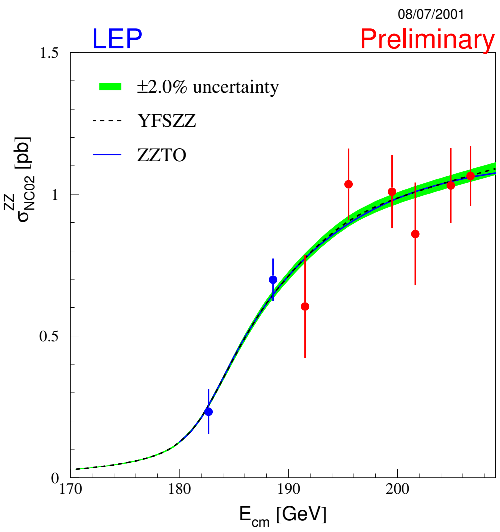

Figure 3. Measurement of the Z-pair cross-section, compared to the predictions of YFSZZ [6] and ZZTO [7].

1.2. Weν

Single-W production is the process where a quasi-real photon, radiated by one of the incoming beams, scatters off the other beam producing a W boson and a neutrino. In terms of 4f final state, the Weν cross-section is defined considering only the gauge invariant set of the t-channel graphs with the addition of cuts, specific of the different final states, to reject the multiperipheral contributions [1]:

- $e^-\bar{\nu}_e q\bar{q}'$ (CC20): $m_{q\bar{q}'} > 45$ GeV;
- $e^-\bar{\nu}_e \ell^+\nu_\ell$ (CC18): $E_{\ell+} > 20$ GeV;
- $e^-\bar{\nu}_e e^+\nu_e$ (Mix56): $E_{e+} > 20$ GeV, $|\cos\theta_{e+}| < 0.95$ and $|\cos\theta_{e-}| > 0.95$.

Theory. A considerable theoretical effort was dedicated in the study of the process. From the technical point of view the process has a collinear singularity which demands a fully massive calculation of the matrix element. From the physics point of view the two main difficulties arise from the different energy scales involved. The first one is the choice of the energy scale for the couplings. In fact when studying high energy processes part of the higher order corrections can be reabsorbed in the Born approximation by using the so-called G_F-scheme, where G_F, M_Z and M_W are input parameters while the weak mixing angle s^2_W and α_{EM} are derived quantities:

$$s^2_W = 1 - \frac{M^2_W}{M^2_Z}, \ \alpha_{EM} = \sqrt{2}\,\frac{G_F M^2_W s^2_W}{\pi}.$$

In the presence of low t-channel scales such an approach fails as the choice $\alpha_{EM}(t \sim 0) = 1/137$ is more appropriate for the t-channel diagrams. The change of the scale $\alpha_{EM}(M^2_W) \to \alpha_{EM}(0)$ leads to a decrease of the cross-section of about 5%. A consistent QFT solution is represented by the Exact Fermion Loop (EFL) calculation [8] which provides a gauge invariant treatment of the finite width of the W boson and allows to properly fix the scale. Approximate solutions exist [9,10], which are in agreement at LEP2 ener-

[1] Charge conjugation is implied.

gies better than 2% with the EFL, and are currently implemented in Monte Carlo generators at disposal of the experiments. The second problem is the treatment of the QED radiation. For a s-channel process, the cross-section is usually obtained from the convolution of a Born cross-section σ_0 with the structure functions $D(q_i^2, x_i)$ of the initial state e^+ and e^-:

$$\sigma = \prod_{i=e^+,e^-} \int dx_i D(q_i^2, x_i)\sigma_0.$$

Factorization could be wrong in the case of a non-annihilation process. Furthermore in the case of single-W an exact $\mathcal{O}(\alpha)$ calculation of the QED corrections, which would allow to properly fix the scale q_i^2 in the structure function, is not yet available. Finally the comparison with the experimental data requires that photons should be generated with some p_t. The change of scale in the structure function $q^2 = s \to q^2 = 0$ increase the cross-section of about 8%.
A 5% overall uncertainty is assigned to the calculated cross-section.
Experiment. The final states experimentally investigated are listed in table 4. Single-W events are typically unbalanced, with a large value of the missing energy. The total cross-section and that of the hadronic channel are combined among the four experiments according to the expected symmetrized statistical error. The combined cross-sections at $\sqrt{s} = 189$ GeV are:

$$\sigma_{e^-\bar{\nu}_e f\bar{f}'} = 0.62 \pm 0.09(\text{stat}) \pm 0.03(\text{syst})\,\text{pb},$$
$$\sigma_{e^-\bar{\nu}_e q\bar{q}'} = 0.46 \pm 0.08(\text{stat}) \pm 0.02(\text{syst})\,\text{pb}.$$

The measured total cross-section as a function of $\sqrt{s}$ together with the theoretical prediction is shown in figure 4.

Table 4
Final states experimentally investigated for Weν.

Final state	Signature	ε
$e^-\bar{\nu}_e q\bar{q}'$	2 acoplanar jets	50%
$e^-\bar{\nu}_e \mu^+\nu_\mu$	1 high p_T track+μ-ID	75%
$e^-\bar{\nu}_e \tau^+\nu_\tau$	1 low multiplicity jet	40%
$e^-\bar{\nu}_e e^+\nu_e$	1 high p_T track+e-ID	75%

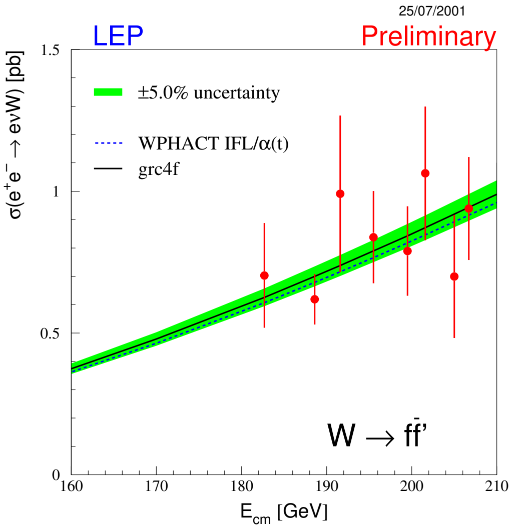

Figure 4. Measurements of the single-W cross-section compared to the predictions of WPHACT [9] and GRC4f [11].

1.3. γ^*/Zee

Single-Z production is the process where a quasi-real photon, radiated by one of the incoming beams, scatters off the other beam producing a γ^*/Z boson and an electron/positron. As in the case of single-W this reaction proceeds through several graphs (48 in the case of an $e^+e^-f\bar{f}$ final state with $f \neq e^-, \nu$ and neglecting the graphs with a Higgs boson exchange) and the experimental definition of the cross-section focuses on the sole t-channel component while reducing the contribution from the multiperipheral graphs. To better separate the γ^* and Z components, two separate cross-sections are given in two ranges of $m_{f\bar{f}}$, above and below 60 GeV. In the region of high invariant mass the expected cross-section is about 1 pb. In contrast to single-W, there is not yet a LEP common definition for the γ^*/Zee cross-section. Therefore up to now there was not a dedicated theoretical effort on this process.

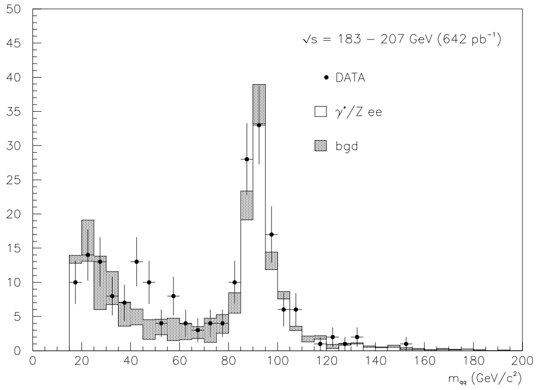

Figure 5. Invariant mass of the hadronic system from DELPHI γ^*/Zee analysis ($m_{\mathrm{q\bar{q}}} > 15$ GeV). The prediction for γ^*/Zee is from GRC4f.

Experiment. Only DELPHI and OPAL have presented γ^*/Zee analyses so far:

- DELPHI: the signal is defined considering all the diagrams but the gamma-gamma multiperipherals and then applying kinematic cuts on the energy E_e and polar angle $\cos\theta_e$ of the tag electron. Two final states have been analyzed, $\mathrm{e^+e^-q\bar{q}}$ and $\mathrm{e^+e^-}\mu^+\mu^-$, and results have been given on the overall LEP2 data sample (about 640 pb^{-1}). The invariant mass distribution of the hadronic system is shown in figure 5.

- OPAL: the signal is defined considering only the t-channel diagrams but all the multiperipherals, and then applying cuts on the Mandelstam variables $\hat{t}, \hat{u}$ and p^2_γ, of the hard process $\mathrm{e}\gamma \to \mathrm{e}\gamma^*/\mathrm{Z}$. Only the $\mathrm{e^+e^-q\bar{q}}$ final state has been investigated on the statistics collected at 183-189 GeV.

Both the experiments find results in agreement with SM expectations.

2. 6f physics

Although there was no evidence at LEP2, 6f final states will be of utmost importance at the forthcoming Linear Collider. A scenario of particular interest will be the existence of a Higgs boson with a mass $m_H \geq 140$ GeV (intermediate mass Higgs), which decays predominantly into a boson pair. In this case at least four fundamental processes will lead to 6f final states:

- intermediate Higgs production,

- $\mathrm{t\bar{t}}$ production,

- WWZ production,

- WW scattering.

Also in the case of 6f physics, several of the most interesting final states offer multiple interpretations. For example the final state $\mu^-\bar{\nu}_\mu\mathrm{u\bar{d}b\bar{b}}$ can be originated either from the process $\mathrm{e^+e^-} \to \mathrm{W^+W^-Z} \to \mu^-\bar{\nu}_\mu\mathrm{u\bar{d}b\bar{b}}$, or from $\mathrm{e^+e^-} \to \mathrm{t\bar{t}} \to \mu^-\bar{\nu}_\mu\mathrm{u\bar{d}b\bar{b}}$ or finally from $\mathrm{e^+e^-} \to \mathrm{ZH} \to \mathrm{W^+W^-Z} \to \mu^-\bar{\nu}_\mu\mathrm{u\bar{d}b\bar{b}}$. Compared to 4f processes, a complete diagrammatic computation of a 6f process involves about 10 times more diagrams and an increase in the number of the dimensions of the phase-space where the amplitudes have to be integrated, including ISR, from 9 to 15. Complete tree-level diagrammatic calculations of some selected final states have been already produced by the authors of the codes SIXPHACT, SIXFAP, GRACE, WIZARD, PANDORA [12]. Comparisons with the results from the Narrow Width Approximation [13], where the calculation is split into the production of resonances and their subsequent decay, show differences up to 10% in the signal graphs and up to 30% in the background ones (i.e. non signal graphs leading to the same 6f final state and their interference with the signal) [14].

3. Conclusions

The measurement of the cross-section of 4f processes represents a relevant LEP legacy. In the scope of 4f physics, processes representing important background to searches were measured, thus enforcing the "no discovery" legacy of LEP. Furthermore processes, which will be those dominant for precision electroweak physics at the Linear Collider, were measured for the first time with an accuracy better than 10%. These measurements stimulated the theoretical community to provide accurate predictions in a wider region of the phase-space, either in form of analytical calculations and in that of events generators.

REFERENCES

1. G. Leibenguth, these proceedings.
2. M. Kienzle-Focacci, these proceedings.
3. F. Boudjema et al., Report on *Standard Model processes* in Vol.1 *Physics at LEP2*, G. Altarelli, T. Sjöstrand and F. Zwirner eds., (1996) CERN 96–01.
4. The LEP collaborations and the LEP WW working group, LEPEWWG/XSEC/2001-03 `http://lepewwg.web.cern.ch/LEPEWWG/lepww`.
5. M.W. Grünewald et al., Report on *Four-fermion production in electron-positron collisions* in *Reports of the working groups on precision calculations for LEP2 physics*, S. Jadach, G. Passarino and R. Pittau eds., (2000) CERN 2000–009.
6. S. Jadach, W. Placzek, B.F.L. Ward, *Phys. Rev.* B56 (1997) 6939.
7. G. Passarino, `http://www.to.infn.it/~giampier/zzto`.
8. G. Passarino, *Nucl. Phys.* B574 (2000) 451; G. Passarino, *Nucl. Phys.* B578 (2000) 3.
9. E. Accomando, A. Ballestrero and E. Maina *Phys. Lett.* B479 (2000) 209.
10. F.A. Berends, C.G. Papadopulos and R. Pittau, *Comput. Phys. Commun.*136 (2001) 148.
11. J. Fujimoto et al., *Comput. Phys. Commun.*100 (1997) 128.
12. Report on e^+ e^- *Linear Colliders: Physics and Detector Studies, Part E*, R. Settles ed., DESY 97-123E (1997);
    E. Accomando et al., *Phys. Rep.* 299 (1998) 1.
13. J. Ellis, M.K. Gaillard and D.V. Nanopuolos, *Nucl. Phys.* B106 (1976) 292;
    J.D. Bjorken, SLAC Report 198.
14. A. Ballestrero, *Acta. Phys. Pol.* B29 (1008) 2811;
    F. Gangemi et al., *Nucl. Phys.* B559 (1999) 3.